

Development of position tracking electric drive system to control BLDC motor working in very low mode for industrial machine application

Pham Van Minh, Tran Duc Chuyen, Dang Quoc Du, Hoang Dinh Co

Faculty of Electrical, University of Economics, Technology for Industries, Ha Noi, Viet Nam

Article Info

Article history:

Received Dec 7, 2022

Revised Jan 11, 2023

Accepted Jan 19, 2023

Keywords:

BLDC

Nonlinear control

Position control

Tracking drive system

Very low speed

ABSTRACT

In this paper, the research and development of kinematic characteristics and models of electromechanical tracking drive systems working in slow mode are presented, applied in industrial, civil, national defense and security machines security, using brushless direct current motors (BLDC). On the basis of building simulation models; then evaluate the speed, rotation angle, torque, and current components for this tracking electric drive system. The simulation model was verified on MATLAB/Simulink, experimented with the model to demonstrate the research results. These research results will be the basis for setting up control algorithms and designing tracking electric drive systems in industry, civil and national defense.

This is an open access article under the [CC BY-SA](#) license.



Corresponding Author:

Tran Duc Chuyen

Faculty of Electrical, University of Economics, Technology for Industries

456 P. Minh Khai, Vĩnh Tuy, Hai Bà Trưng, Ha Noi, Viet Nam

Email: tdchuyen@uneti.edu.vn

1. INTRODUCTION

In recent years, brushless DC motors (BLDC) are being widely used in high quality speed regulated traction electric drive systems. This electric drive system is widely used in high-precision technical equipment such as electric vehicles, industrial robot soft joints, industrial electric drive systems, weapon tracking systems, military, laser rangefinders, ground and aircraft radar systems and medical equipment. Due to the BLDC engine having its outstanding characteristics (wide operating speed range, large torque/current ratio, low noise, stable, high efficiency, direct torque control and large current) [1]–[5]. The tracking electric drive system works in slow mode (the engine rotation speed is very low and corresponds to a small setting angle, there is always a different variation) this is a complex system that requires a traction output signal. closely follow the input signal with a small amount of error, when the input signal has variable error [5]–[7]. We always want this error to be as small as possible, depending on the requirements of the control device of the electric drive system [8], [9]. In Figure 1, the electric drive system tracking the angle; where, the input signal to the system is (X_v), the output signal is the output response according to the rotation angle (X_r).

In electromechanical tracking drive systems that require small tracking errors, the motion properties of the system must be taken into account in the design of the regulator, [10]–[12]. With high-speed motion, the actuator motor's rotational torque is many times larger than the frictional torque, with slow-speed motion, the actuator motor's torque allows comparison with the frictional and resistance torques, [2], [6]. When considering working at slow and very slow speeds, the quality of adhesion depends on many uncertain nonlinear factors: damping moment, elasticity of the flexible coupling and due to clearance [8], [10], [13]. The construction of a simulation model for this transmission system is of great significance in building a torque and speed control loop to ensure optimal fast-acting for the system during control [14]–[16].

This paper presents a method to simulate the electromechanical system working at slow speed to ensure torque, combined with proportional correction-PI integral to correct angular deviation, experiment with simulation model figures and measuring devices; hardware control for the object to demonstrate the results [17]–[21]. The research results will be the basis for setting up control algorithms and designing traction drive systems in industry and defense scientific research interest [22]–[25].

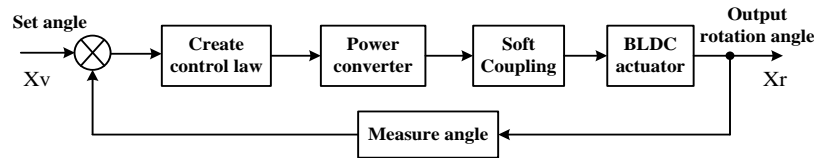


Figure 1. The model control of electromechanical tracking drive system by angle

2. CONTENTS OF RESEARCH PROPOSAL

2.1. Momentation of the systemization of the transport system bytes of slow speed

When designing the tracking system, it is often assumed that the resistance torque characteristics are the torque components acting on the engine's rotational shaft; is a nonlinear component that is difficult to determine. When the motor is loaded, the speed decreases as the load increases. The property of the resisting moment can exist in two forms: the frictional moment and the mechanical moment [2], [3], [8], [16], [19], [26]. We calculate the resisting moment due to friction of the form (1).

$$M_{C.T} = -M_{C.T1}^0 \text{sign}\omega \text{ with } \omega \neq 0 \quad (1)$$

This assumption is only true when the drive system is operating at high speed. In many cases, the tracking system is required to work with high accuracy at low or very low speeds. Then the damping moment characteristic has the form Figure 2(a) and Figure 2(b) it has a segment with negative derivative [16], [20].

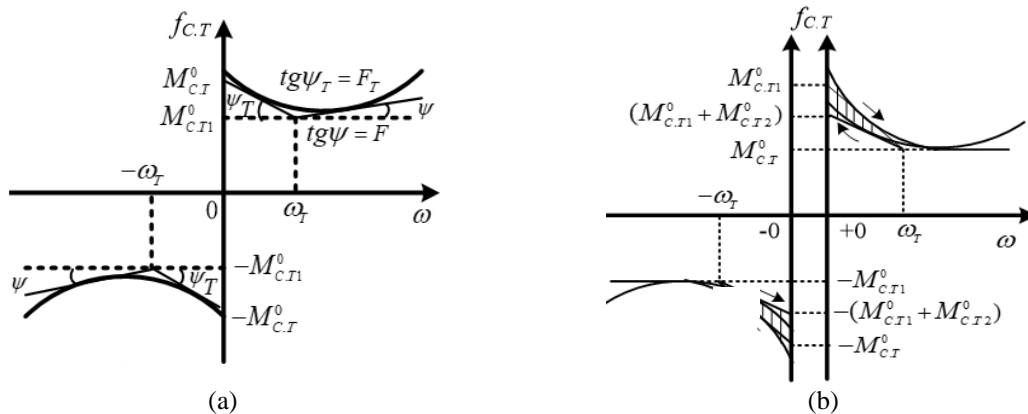


Figure 2. Load torque characteristics of the tracking drive system operating at slow speeds
(a) with the characteristic of changing frictional moment (calculated by phase angle) and
(b) when changing the direction of motion through the speed value zero

Asymptote to the characteristic curve change of frictional resistance moment equal to the tangent line, we have:

$$M_{C.T}(\omega) = - \begin{cases} (M_{C.T}^0 - F_T|\omega|)\text{sign}\omega; 0 < |\omega| < \omega_T \\ (M_{C.T1}^0 - F|\omega|)\text{sign}\omega; |\omega| \geq \omega_T \end{cases} \quad (2)$$

in which, M_{CT} ; F_T ; F , ω_T are constants; ω rotational speed of the motor. For the hysteresis characteristic of the frictional moment, we can asymptotically use the (3).

$$f_{c.T}(\omega) = f_{c.T1}(\omega) + f_{c.T2}(\omega) + f_{c.T3}(\omega), \quad (3)$$

Where component $f_{c.T1}(\omega) = M_{c.T1}^0 \text{sign}\omega$ is the dry friction moment characteristic; $f_{c.T2}(\omega)$ is the characteristic of the moment of friction with a negative derivative, $F_{T2} = dM_{c.T2}/d\omega$.

$$f_{c.T2}(\omega) = - \begin{cases} (M_{c.T2}^0 - F_{T2}|\omega|)\text{sign}\omega; 0 < |\omega| < \omega_T, \omega\dot{\omega} > 0; \\ 0|\omega| \geq \omega_T, \omega\dot{\omega} < 0. \end{cases} \quad (4)$$

$f_{c.T3}(\omega)$ is the form of frictional moment characteristic with a negative derivative, $F_{T3} = \frac{dM_{c.T3}}{d\omega}$

$$f_{c.T3}(\omega) = - \begin{cases} (M_{c.T3}^0 - F_{T3}|\omega|)\text{sign}\omega; 0 < |\omega| < \omega_T, \omega\dot{\omega} < 0; \\ 0|\omega| \geq \omega_T, \omega\dot{\omega} < 0. \end{cases} \quad (5)$$

The first two terms of (3) determine the unvalued property of the function $F_{c.T}(\omega)$ Figure 2(a). the third term takes into account the characteristic of $F_{c.T3}(\omega)$, it depends on direction and speed of the actuating motor shaft [6], [7]. When the motor shaft stops ($\omega = 0$) the resistance torque in (2) is determined by the static frictional torque, which takes the value in the range:

$$-M_{c.T}^0 \leq M_{c.T}(0) \leq M_{c.T}^0, \quad (6)$$

When the traction system is working at slow mode, the influence of the frictional moment component is significant. When the friction torque model is combined between the viscous friction component and the dry friction component: viscous friction can be easily described using the reactive coefficient; Dry friction in the system is dependent on the quality of the contact surface. The static models of the frictional moment components do not fully describe the dynamic effects of the friction process such as: displacement before sliding, hysteresis characteristics; stribek effect, low speed and pre-slip zone. With the goal of precise control of position and tracking problem at very low speed, then people use dynamic friction torque model: In fact, there is Dahl model; and LuGre model, [11], [12]. Change characteristics of $M_{c.T}(0)$ Figure 2(b). When changing the direction of motion through the value 0 specified by the (7).

$$-M_{c.T}^0 \leq M_{c.T}(0) \leq M_{c.T1}^0 + M_{c.T2}^0, \quad (7)$$

Then the speed changes from positive to negative and we have:

$$-(M_{c.T}^0 + M_{c.T2}^0) \leq M_{c.T}(0) \leq M_{c.T}^0 \quad (8)$$

The process is reversed when the speed changes from negative to positive. In the above formulas the component $M_{c.T1}^0, M_{c.T2}^0, M_{c.T3}^0$ and the slope coefficients F_{T2}, F_{T3} is constant.

Figure 2(b) shows a graph of $f_{c.T}(\omega)$ when there is a delay. It has two branches; a branch corresponding to the case when speed; increases to a speed exceeding ω_T . The second branch corresponds to the case of changing the direction of motion. If the rate ω changes within a limit less than ω_T , then we assume that the graph $f_{c.T}(\omega)$ in the lagging branch has a vertical segment.

With the above torque characteristic, when the tracking drive system works at low speed, oscillations may arise. Suppose the motion speed of the control object consists of two components: a constant component ω_0 and a harmonic variable component $\omega_r(t) = \omega_a \sin \omega t$.

$$\omega(t) = \omega_0(t) + \omega_r(t) \quad (9)$$

For the impact on $\beta(t)$ and the slow-varying noise moment $M_B(t)$, we have:

$$|\dot{\beta}(t)| \gg |\dot{\beta}(t + 2\pi/\omega) - \dot{\beta}(t)|; |M_B(t)| \gg |M_B(t + 2\pi/\omega) - M_B(t)|.$$

It can be said that in one oscillation period of $\omega_r(t), \beta, \omega_0, M_B, \omega_a$ and ω are constant. Oscillation $\omega_r(t)$ is high frequency compared to $\beta(t)$ and $M_B(t)$. Using harmonic linearization method to determine amplitude and phase of first-order harmonic with resistance moment component $M_{c.T}(t)$. Expanding the function $f_{c.T}(t)$ according to the Furie series, ignoring the higher order harmonic terms, we get the expression of the resistance moment on the output of the nonlinear element as shown in Figure 2(a).

$$M_{C.T}(t) = -f_{C.T}(t) = -[M_{C.T0}(\omega_a, \omega_0) + q(\omega_a, \omega_0)\omega_r(t)], \quad (10)$$

When the characteristic has the form of Figure 2(b), we have:

$$M_{C.T}(t) = -f_{C.T}(t) = -\left\{M_{C.T0}(\omega_a, \omega_0) + [q(\omega_a, \omega_0) + \frac{q'(\omega_a, \omega_0)}{\omega}p]\omega_r(t)\right\}, \quad (11)$$

here $M_{C.T0}$: constant component; $q(\omega_a, \omega_0)$, $q'(\omega_a, \omega_0)$ harmonic linearization coefficient. In (10) and (11) can be written in the form:

$$M_{C.T}(t) = -[M_{C.T0}(\omega_a, \omega_0) + W_H(\omega_a, \omega_0)\omega_r(t)], \quad (12)$$

here, $WH(\omega_a, \omega_0)$ is a nonlinear element transfer function as shown in Figure 2 with the input as the harmonic signal $\omega_r(t)$ and the output as the first order harmonic function of $f_{C.T}(t)$. With a single-valued nonlinear element as shown in Figure 2(a), we have:

$$W_H(\omega_a, \omega_0) = q(\omega_a, \omega_0), \quad (13)$$

with the nonlinear element with hysteresis Figure 2(b), we have:

$$W_H(\omega_a, \omega_0) = q(\omega_a, \omega_0) + \frac{q'(\omega_a, \omega_0)}{\omega}p, \quad (14)$$

from the (9) with the function $f_{C.T}(t)$ according to (10), (11) we have:

$$M_{C.T0}(\omega_a, \omega_0) = \frac{1}{2\pi} \int_0^{2\pi} M_{C.T}(\omega_0 + \omega_a \sin \gamma) d\gamma; \quad (15)$$

$$q(\omega_a, \omega_0) = \frac{1}{\omega_a \pi} \int_0^{2\pi} M_{C.T}(\omega_0 + \omega_a \sin \gamma) \sin d\gamma; \quad (16)$$

$$q'(\omega_a, \omega_0) = \frac{1}{\omega_a \pi} \int_0^{2\pi} M_{C.T}(\omega_0 + \omega_a \sin \gamma) \cos d\gamma, \quad (17)$$

here, $\gamma = \omega t$; where t is the time from the beginning of an oscillation period [16]–[18], [24]–[26]. On the basis of the kinematic characteristics of the slow-speed tracking system, we build a model for the tracking system using the BLDC motor in Figure 1.

2.2. Building a controller model for a BLDC motor

DC motors have superior control performance compared to other types of motors, but the existence of a brush commutator reduces its reliability and applicability. The BLDC motor was born as a combination of synchronous motor with semiconductor switch by BJTs (Bipolar junction transistor, two-junction transistor: MOSFET, JFET, IGBT), which has combined overdrive control feature. Outstanding with high reliability is a good alternative to DC motors in weapons control systems and in industry; requires high quality. In essence, the model of the BLDC motor is a rather complex intermittent model. In the electric drive systems of small and medium power automation systems, there are mainly permanent magnet excitation motors.

The BLDC motor is considered here in a combination of: rotor position sensor, converter block and power semiconductor circuit part. They form and feed the stator windings of 3-phase motors; voltages V_a , V_b , V_c are suitable for the rotor position [1], [2], [9]. In rotor flux-based control, torque and flux are controlled independently, so the angular position and speed of the rotor are essential information in the control design. Therefore, position sensors with high resolution are often used to locate rotors and power semiconductor switches, which interact with the excitation magnetic field to produce rotational torque. Furthermore, in the low-speed working domain of this traction system, it is necessary to measure the position and speed of the rotor precisely with the position sensor mounted on the motor shaft, which plays the role of very important in the control loop circuit besides adjusting the speed and position also need to adjust the torque [1], [2], [4], [8], [10], [12].

From there, we will consider: The model of the drive system following the angle with the BLDC actuator working at slow speed as shown in Figure 3(a), and the structure of the stator and rotor windings as permanent magnets is shown as shown in Figure 3(b). The mathematical model of the BLDC motor in this paper is a three-phase, four-pole connected star as shown in Figure 3(a). Therefore, the model of changing the voltage components of the phases abc is the model represented by the d-q coordinate system. Furthermore, the following assumptions are made: The stator resistance, the mutual inductance values between the phases are equal and constant; Hysteresis and eddy current losses are eliminated; All power switches are considered ideal [4], [10], [22]. With such assumptions, the mathematical model of the BLDC motor in Figure 3 is described as follows:

$$V_a = R_a i_a + L_a \frac{di_a}{dt} + M_{ab} \frac{di_b}{dt} + M_{ac} \frac{di_c}{dt} + E_a \quad (18)$$

$$V_b = R_b i_b + L_b \frac{di_b}{dt} + M_{ba} \frac{di_a}{dt} + M_{bc} \frac{di_c}{dt} + E_b \quad (19)$$

$$V_c = R_c i_c + L_c \frac{di_c}{dt} + M_{ca} \frac{di_a}{dt} + M_{cb} \frac{di_b}{dt} + E_c \quad (20)$$

Where, R_a, R_b, R_c is armature of each phase [Ω]; L_a phase armature inductance [H]; M_{ab}, M_{bc}, M_{cb} mutual support between phases; V_a, V_b, V_c each phase voltage [V]; E_a, E_b, E_c phase electromotive force (back-EMF) [V]. Then we have:

$$E_a = K_e \omega_m F(\theta_e); E_b = K_e \omega_m F(\theta_e - 2\pi/3); E_c = K_e \omega_m F(\theta_e + 2\pi/3) \quad (21)$$

where, K_e is the electromotive force constant [V/rad. s^{-1}], $F(\theta_e)$ function of the electromotive force coefficient of the motor rotor position, θ_e the electromotive force angular constant of the rotor; ω_m rotor angular speed [rad. s^{-1}]; and we have (22).

$$\omega_m = \frac{d\theta_m}{dt} \quad (22)$$

Therefore, the mathematical model of the BLDC motor can be written as a matrix as (23).

$$\begin{bmatrix} L_a & M_{ab} & M_{ca} \\ M_{ba} & L_b & M_{bc} \\ M_{ca} & M_{cb} & L_c \end{bmatrix} \frac{d}{dt} \begin{bmatrix} i_a \\ i_b \\ i_c \end{bmatrix} = \begin{bmatrix} v_a \\ v_b \\ v_c \end{bmatrix} - \begin{bmatrix} R_a & 0 & 0 \\ 0 & R_b & 0 \\ 0 & 0 & R_c \end{bmatrix} \begin{bmatrix} i_a \\ i_b \\ i_c \end{bmatrix} - \begin{bmatrix} e_a \\ e_b \\ e_c \end{bmatrix} \quad (23)$$

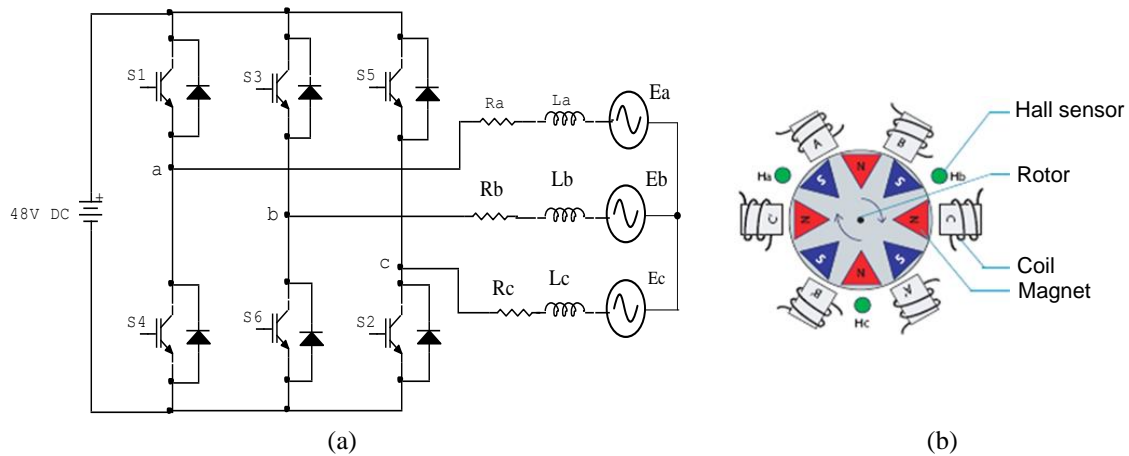


Figure 3. Building a mathematical model of the BLDC motor: (a) model of BLDC motor and (b) location of Hall sensor to measure voltage and torque values

If it is assumed that the rotor is designed on a smooth flat surface, now BLDC motors are generally without undulation [1, 10], so that the motor stator inductance electromotive force does not depend on rotor positions, so: $L_a = L_b = L_c = L$. And the mutual inductance will take the form: $M_{ab} = M_{ac} = M_{ba} = M_{bc} = M_{ca} = M_{cb} = M$. Assume a balanced 3-phase voltage The resistance of the phases is written by: $R_a = R_b = R_c = R$. From that, we rewrite (6) as (24).

$$\begin{bmatrix} L & M & M \\ M & L & M \\ M & M & L \end{bmatrix} \frac{d}{dt} \begin{bmatrix} i_a \\ i_b \\ i_c \end{bmatrix} = \begin{bmatrix} v_a \\ v_b \\ v_c \end{bmatrix} - \begin{bmatrix} R & 0 & 0 \\ 0 & R & 0 \\ 0 & 0 & R \end{bmatrix} \begin{bmatrix} i_a \\ i_b \\ i_c \end{bmatrix} - \begin{bmatrix} e_a \\ e_b \\ e_c \end{bmatrix} \quad (24)$$

Electromagnetic torque generated by the actuator. Here, the actuator motor in this traction system is BLDC, in some studies people ignore the actuator's kinematics [1], [11]; When taking into account the

kinematics of the actuator, the order of the system increases. In order to improve the quality of tracking, it is necessary to consider the kinematics of the actuator, which is the kinematics of the process of generating electromagnetic torque under the input action. For motors that are commutator-free DC motors due to their very good torque characteristics, the input effects are armature voltages across the motor phases, field voltages, or both [2]–[4], [9]. Equation of electromagnetic torque generated by phases of BLDC actuator [5]:

$$\tau_a = K_t i_a F(\theta_e); \tau_b = K_t i_b F(\theta_e - 2\pi/3); \tau_c = K_t i_c F(\theta_e + 2\pi/3) \quad (25)$$

where, K_t is the motor torque constant; i_a, i_b, i_c motor current per phase (A). And then we have:

$$\theta_e = (P/2) \cdot \theta_m \quad (26)$$

when converting to the rotation axis of the working mechanism through the flexible coupling in Figure 1, we have the relationship between the working torque and the electromagnetic torque as follows [5], [9]:

$$\tau_{ct} = K_{ct} \cdot \tau_{motor} \quad (27)$$

where, K_{ct} is the conversion coefficient between the electromagnetic moment and the torque on the shaft of the working structure. Electromagnetic torque generated by BLDC motor [5], [9]:

$$\tau_e - \tau_L = J \frac{d^2 \theta_m}{dt^2} + \beta \frac{d\theta_m}{dt} \quad (28)$$

however, the electromagnetic torque of the three phase BLDC motor is dependent on the current, speed, and feedback electromotive force waveform, so the instantaneous electromagnetic torque at time is written as (29):

$$\tau_{em} = \frac{1}{\omega_m} (E_a i_a + E_b i_b + E_c i_c) \quad (29)$$

or we can also write the electromagnetic torque according to the phases of the BLDC motor:

$$\tau_e = \tau_a + \tau_b + \tau_c \quad (30)$$

where, θ_m mechanical slope of the rotor [rad]; τ_e electromagnetic torque generated by the actuator motor [Nm]; J moment of inertia [kgm^2]; β frictional moment constant [$\text{Nms} \cdot \text{rad}^{-1}$]; τ_L drag torque depends on the load [Nm].

From (18), (19), (20) and (28) we can also write the following:

$$V_{ab} = R(i_a - i_b) + (L - M) \frac{d}{dt}(i_a - i_b) + E_{ab} \quad (31)$$

$$V_{bc} = R(i_b - i_c) + (L - M) \frac{d}{dt}(i_b - i_c) + E_{bc} \quad (32)$$

where, $i_a + i_b + i_c = 0$, so after transforming (31) and (32) and ignoring the mutual induction coefficients between the phases we have:

$$\frac{di_a}{dt} = -\frac{R}{L} i_a + \frac{2}{3L} (V_{ab} - E_{ab}) + \frac{1}{3L} (V_{bc} - E_{bc}) \quad (33)$$

$$\frac{di_b}{dt} = -\frac{R}{L} i_b - \frac{2}{3L} (V_{ab} - E_{ab}) + \frac{1}{3L} (V_{bc} - E_{bc}) \quad (34)$$

From that, the state space model of the BLDC motor is written as (35).

$$\begin{bmatrix} i'_a \\ i'_b \\ \omega'_m \end{bmatrix} = \begin{bmatrix} -\frac{R}{L} & 0 & 0 \\ 0 & -\frac{R}{L} & 0 \\ 0 & 0 & -\frac{\beta}{L} \end{bmatrix} \begin{bmatrix} i_a \\ i_b \\ \omega_m \end{bmatrix} + \begin{bmatrix} \frac{2}{3L} & \frac{1}{3L} & 0 \\ -\frac{1}{3L} & \frac{1}{3L} & 0 \\ 0 & 0 & \frac{1}{J} \end{bmatrix} \begin{bmatrix} V_{ab} - E_{ab} \\ V_{bc} - E_{bc} \\ \tau_e - \tau_L \end{bmatrix} \quad (35)$$

Finally, then we have (36).

$$\begin{bmatrix} i_a \\ i_b \\ i_c \\ \omega_m \end{bmatrix} = \begin{bmatrix} 1 & 0 & 0 \\ 0 & 1 & 0 \\ -1 & -1 & 0 \\ 0 & 0 & 1 \end{bmatrix} \begin{bmatrix} i_a \\ i_b \\ i_c \\ \omega_m \end{bmatrix} \quad (36)$$

The expansion of the state space model of the BLDC motor according to (35), (36) makes it easier to calculate and build a simulation model of this electromechanical system.

3. THE SIMULATION AND EXPERIMENTAL RESULTS

On the basis of the theory given above, the authors conducted simulations and experiments at the Department of Industrial Electricity, Faculty of Electrical Engineering; University of Economics-Industrial Engineering, with full equipment: Engines, embedded computers with high configuration (Core i7-6600U/16 GB Ram/512 GB SSD/8 GB HD Graphics 520 Card), MATLAB/Simulink R2021 incorporates a on chip TMS230 series DSP embedded hardware control card that is inserted into the circuit that the research team designed and manufactured as a drive, instrumentation for measuring, switching and protecting the test system. On the basis of the built model and the mathematical equations of the BLDC motor given above, the control law has been built assuming all state variables can be measured in the experimental process. The simulation parameters of the Japanese BLDC motor are as follows: speed is 3000 rpm; $p = 4$; phase number is 3; DC power source is 48 V to 60 V; rated current is 50 A, $P = 300$ (W); $J = 0.8e^{-3}$ (kgm^2); $R = 2.8750\Omega$; $L_s = 8.5e^{-3}$ (H); torque is 5 Nm.

The selection of sensors for tracking transmissions working near zero and zero speed over the entire speed range with high accuracy requirements, commonly used sensors are Hall sensors and encoder with angular position output sine cos; or in arctan (sin/cos). This is necessary to allow adjustment of the mechanisms of the torque control ring as well as the position and speed control rings [2], [9], [12]. On that basis, we have simulation results with different input amounts according to (preset angle). System survey taking into account the influence of regulator parameters on the quality of the system; fast acting and the ability to asymptotically (stick) without oscillation to the end position, from which to choose the parameter of the regulator to achieve the desired value with the smallest error.

Case 1: Simulates a speed of 1000 rpm applied to the process of turning on the machine shown in Figure 4 and changing the speed from 1000 rpm to -1000 rpm as shown in Figure 5 in a period of 1 second; The response of the output system always follows the input during the working process as shown in Figure 4 and Figure 5.

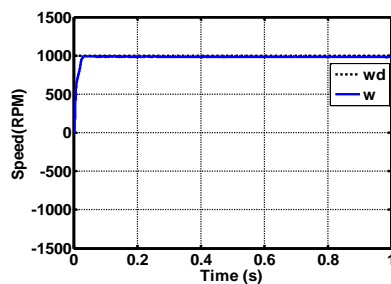


Figure 4. 1000 rpm speed response in case 1

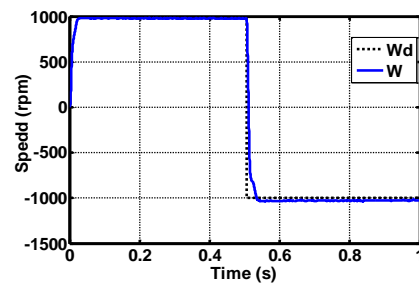


Figure 5. Speed response when varying from 1000 rpm to -1000 rpm in case 1

Case 2: Simulation at a low speed of 50 rpm for a 1 second response time the traction drive system always responds to the initial set value in Figure 6. When the working speed is as low as 30 rpm, the response time is 1.5 seconds; the process of changing the speed from 30 rpm to -30 rpm, the output response of the traction drive system always adheres to the set value during working, the system works well, as shown in Figure 7.

Case 3: Simulation with the position controller of the drive system in the case that the angle applied to the system is 0.1 rad in the response time of 1 second as shown in Figure 8 and the case when the angle is greater than 0.58 rad in the time response 1.5 seconds as shown in Figure 9; we see that the system works stably, the output follows the input, and the control quality is high enough to meet the needs of industry and military.

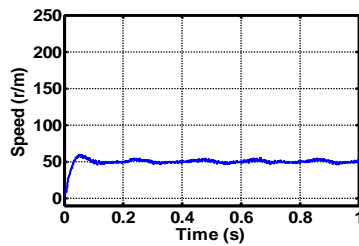


Figure 6. Low speed response at 50 rpm in the case 2

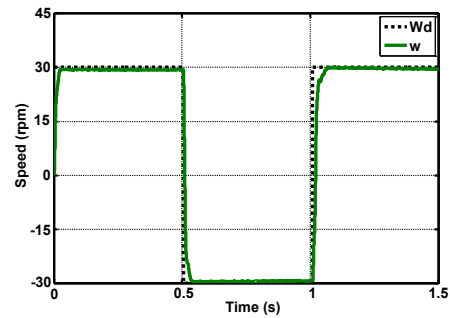


Figure 7. Speed response with 30 rpm in the case 2

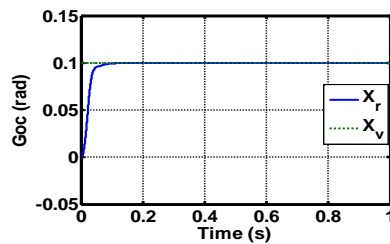


Figure 8. Input/output response at 0.1 rad in case 3

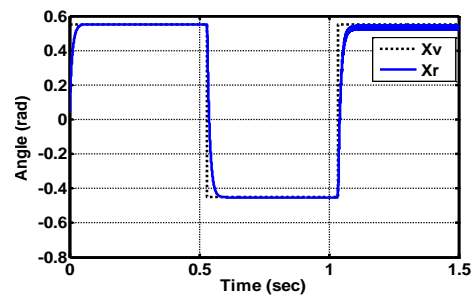
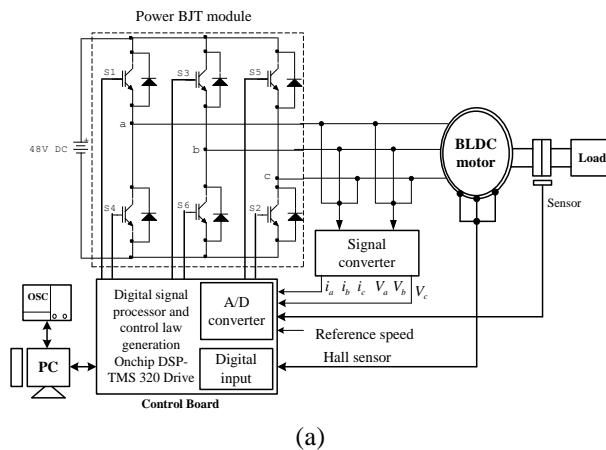
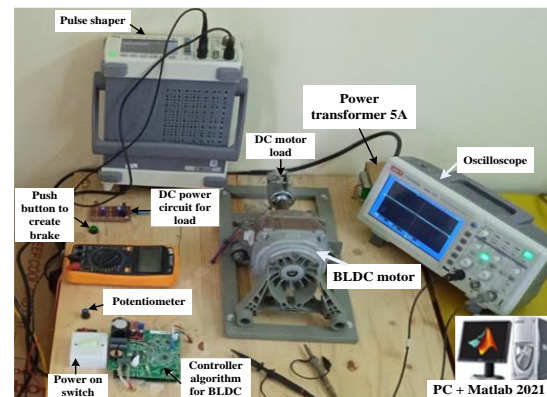


Figure 9. Input/output response at 0.58 rad in case 3



(a)



(b)

Figure 10. The overall system in experimental: (a) control diagrams and (b) the experimental system

Experiment with the structural diagram as shown in Figure 10(a) and experimental model as shown in Figure 10(b). Experimental parameters include: controller built with onchip DSP board of TMS 320 series which is considered as a Drive set, BLDC motor parameters as shown in simulation, DC motor used to generate load, in addition, there are power supply boards and measuring devices and computers for experimentation. Compared with the results in [16], [22], [24] the results of the paper have better quality than the simpler control system, which is also a basis for building some newer algorithms.

Then we have the following experimental results: Figure 11 is the response of the controller to the output voltage of the torque-stabilized BLDC motor. Current value according to the speed of the BLDC motor working at very low speed, from near zero and through zero (up to 50 rpm). In Figure 11 respectively, the response from the controller model of the tracking system using a BLDC motor with parameters as shown in the simulation, the BLDC motor works at low speed: speed 50 rpm/min \rightarrow 5 v/div; torque 5Nm; phase current 4 A/div, and speed 20 rpm/min \rightarrow 5 v/div; phase current 4 A/div. In Figures 11(a) and 11(b), the responses are: i) torque, ii) current is 2.5 A, and iii) voltage 30 v/div and working speed of BLDC motor. In total response time is 5 ms.

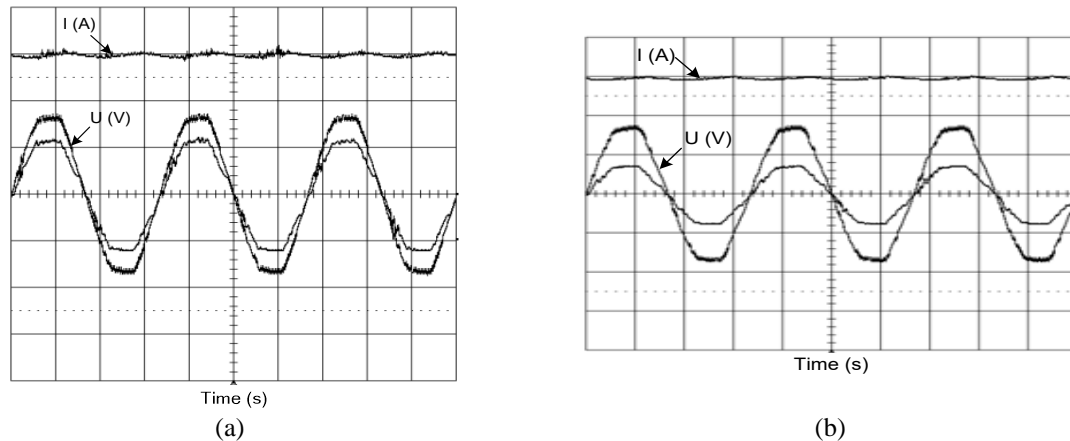


Figure 11. Experimental results of control system using BLDC motor: (a) response working speed when speed value 50 rpm/min and (b) response working speed when speed value 20 rpm/min

4. CONCLUSION

The research results of this paper are based on theoretical basis, mathematical model of BLDC motor, experimental simulation of electric drive system with angular grip to control BLDC motor working in very low speed for application in military industrial machines. The process of saving this electromechanical system has many outstanding advantages compared to transmission systems using asynchronous and DC motors. This is a drive system with many advantages: high efficiency, no losses in the rotor, smaller no-load current due to strong permanent magnets, control characteristics less sensitive to motor parameter variations, the regulation of speed, torque and current is superior to other types of motors in industry and military.

ACKNOWLEDGEMENTS

This research was supported by Faculty of Electrical Engineering, University of Economics-Technology for Industries, Viet Nam.




REFERENCES

- [1] A. Emadi, "Advanced electric drive vehicles," *Advanced Electric Drive Vehicles*, 2014, doi: 10.1201/9781315215570.
- [2] N. P. Quang and J. A. Dittrich, "Vector Control of Three-Phase AC Machines: System Development in the Practice," *Power Systems*, vol. 20, 2008.
- [3] J. Chiasson, "Modeling and high performance control of electric machines," (*IEEE Press Series on Power Engineering*), 2005.
- [4] J. Connor and S. Laflamme, "Advanced Control Theory," *Structural Motion Engineering*, pp. 545–599, 2014, doi: 10.1007/978-3-319-06281-5_10.
- [5] A. Bacciotti, "Stability and control of linear systems," *Studies in Systems, Decision and Control*, vol. 185, pp. 1–189, 2019, doi: 10.1007/978-3-030-02405-5_1.
- [6] A. K. M. Arafat and S. Choi, "Optimal phase advance under fault-tolerant control of a five-phase permanent magnet assisted synchronous reluctance motor," *IEEE Transactions on Industrial Electronics*, vol. 65, no. 4, pp. 2915–2924, 2018, doi: 10.1109/TIE.2017.2750620.
- [7] K. M. Arun Prasad and U. Nair, "Intelligent fuzzy sliding mode controller based on FPGA for the speed control of a BLDC motor," *International Journal of Power Electronics and Drive Systems*, vol. 11, no. 1, pp. 477–486, 2020, doi: 10.11591/ijpeds.v11.i1.pp477-486.
- [8] M. Jufer, "Electric Drives," *Electric Drives*, 2013, doi: 10.1002/9781118622735.
- [9] K. D. Pham and N. Van Nguyen, "A reduced common-mode-voltage pulsewidth modulation method with output harmonic distortion minimization for three-level neutral-point-clamped inverters," *IEEE Transactions on Power Electronics*, vol. 35, no. 7, pp. 6944–6962, Jul. 2020, doi: 10.1109/TPEL.2019.2959984.
- [10] M. Steinberger, M. Horn, and L. Fridman, "Variable-structure systems and sliding-mode control: from theory to practice," 2021.
- [11] L. Keviczky, R. Bars, J. Hetthéssy, and C. Bányász, "Control engineering: MATLAB exercises," *Advanced Textbooks in Control and Signal Processing*, pp. 1–275, 2019, doi: 10.1007/978-981-10-8321-1.
- [12] J. M. Lazi, Z. Ibrahim, M. Talib, A. Alias, A. Nur, and M. Azri, "Speed and position estimator of for sensorless PMSM drives using adaptive controller," *International Journal of Power Electronics and Drive Systems (IJPEDS)*, vol. 10, no. 1, p. 128, 2019, doi: 10.11591/ijpeds.v10.i1.pp128-136.
- [13] M. D. K. M. and L. M., "Sequence prediction of firing angle BLDC motor drive using lookup table," *International Journal of Trend in Scientific Research and Development*, vol. Volume-2, no. Issue-3, pp. 1638–1645, 2018, doi: 10.31142/ijtsrd11514.
- [14] V. J. Pyrhönen and H. S. Semken, "Electrical machine drives control," 2016, p. 527, 2016.
- [15] A. H. Niasar and A. H. Sabbaghean, "Design and implementation of a low-cost maximization power conversion system for brushless DC generator," *Ain Shams Engineering Journal*, vol. 8, no. 4, pp. 571–580, 2017, doi: 10.1016/j.asej.2015.11.001.
- [16] M. S. Zaky, M. Khater, H. Yasin, and S. S. Shokralla, "Very low speed and zero speed estimations of sensorless induction motor drives," *Electric Power Systems Research*, vol. 80, no. 2, pp. 143–151, 2010, doi: 10.1016/j.epsr.2009.07.012.




- [17] N. T. Phuong Chi, D. T. Thao, and T. N. Anh, "Real-time speed control of brushless DC motor based on PID controller," *International Journal of Electrical and Electronics Engineering*, vol. 5, no. 5, pp. 1–5, 2018, doi: 10.14445/23488379/ijeee-v5i5p101.
- [18] H. H. Choi, J. W. Jung, and T. H. Kim, "Digital speed regulator system design for a permanent magnet synchronous motor," *Journal of Electrical Engineering and Technology*, vol. 7, no. 6, pp. 911–917, 2012, doi: 10.5370/JEET.2012.7.6.911.
- [19] T. D. Chuyen *et al.*, "Improving control quality of PMSM drive systems based on adaptive fuzzy sliding control method," *International Journal of Power Electronics and Drive Systems*, vol. 13, no. 2, pp. 835–845, 2022, doi: 10.11591/ijpeds.v13.i2.pp835-845.
- [20] M. Zaky, E. Touti, and H. Azazi, "Two-degrees of freedom and variable structure controllers for induction motor drives," *Advances in Electrical and Computer Engineering*, vol. 18, no. 1, pp. 71–80, 2018, doi: 10.4316/AECE.2018.01009.
- [21] S. K. Kim, K. G. Lee, and K. B. Lee, "Singularity-free adaptive speed tracking control for uncertain permanent magnet synchronous motor," *IEEE Transactions on Power Electronics*, vol. 31, no. 2, pp. 1692–1701, 2016, doi: 10.1109/TPEL.2015.2422790.
- [22] T. Kim, H. W. Lee, and M. Ehsani, "Position sensorless brushless DC motor/generator drives: Review and future trends," *IET Electric Power Applications*, vol. 1, no. 4, pp. 557–564, 2007, doi: 10.1049/iet-epa:20060358.
- [23] D. Czerwinski, J. Gęca, and K. Kolano, "Machine learning for sensorless temperature estimation of a bldc motor," *Sensors*, vol. 21, no. 14, 2021, doi: 10.3390/s21144655.
- [24] A. Sikora and M. Woźniak, "Impact of current pulsation on BLDC motor parameters," *Sensors (Switzerland)*, vol. 21, no. 2, pp. 1–18, 2021, doi: 10.3390/s21020587.
- [25] D. H. Lee, "Wide-range speed control scheme of BLDC motor based on the hall sensor signal," *Journal of Power Electronics*, vol. 18, no. 3, pp. 714–722, 2018, doi: 10.6113/JPE.2018.18.3.714.
- [26] K. Smółka, A. Firyck-Nowacka, and S. Wiak, "Comparison of the Design of 3-Pole BLDC Actuators/Motors with a Rotor Based on a Single Permanent Magnet," *Sensors*, vol. 22, no. 10, 2022, doi: 10.3390/s22103759.

BIOGRAPHIES OF AUTHORS






Pham Van Minh    was born in 1989. He graduated as an Engineer of Electrical Engineering and Technology, majoring in Automation at University of Economic and Industrial Technology. Received a master's degree in Control Engineering and Automation from the University of Transport and Communications, 2014. From 2012 until now he has been a lecturer in Industrial electricity, Faculty of Electrical, University of Economics-Technology for Industries; Ministry of Industry and Trade the socialist republic of Viet Nam. Main research direction: Intelligent control, power electronics. He can be contacted at email: pvmnh@uneti.edu.vn.






Tran Duc Chuyen    received the Ph.D degree in Industrial Automation from Le Qui Don Technical University (MTA), Hanoi, Vietnam in 2016. Now, works at Faculty of Electrical Engineering, University of Economics-Technology for Industries. He is currently the President of Council the Science of Faculty of Electrical Engineering. Dr Tran Duc Chuyen's main researches: Electric machine, drive system, control theory, power electronics and application, adaptive control, neural network control, automatic robot control, motion control, Artificial intelligence. He can be contacted at email: tdchuyen@uneti.edu.vn.



Dang Quoc Du    was born in Nam Dinh. He graduated as an electrical engineering at Hanoi University of Science and Technology, Hanoi, Vietnam, in 2008. He graduated with a Master of Electrical Engineering from Hanoi University of Science and Technology, Vietnam in 2016. Since 2022, he is a lecturer at the Faculty of Electrical Engineering, University of Economics-Industrial Technology; Ministry of Industry and Commerce Vietnam. The main research direction: Intelligent control, Electric machine drives, and renewable energy conversion systems. He can be contacted at email: dqdu@uneti.edu.vn.



Hoang Dinh Co    received the Ph.D degree in Industrial Automation from Le Qui Don Technical University (MTA), Hanoi, Vietnam in 2016. Now, works at Faculty of Electrical Engineering, University of Economics-Technology for Industries. He is currently the President of Council the Science of Faculty of Electrical Engineering. Dr Tran Duc Chuyen's main researches: Electric machine, drive system, control theory, power electronics and application, adaptive control, neural network control, automatic robot control, motion control, Artificial intelligence. He can be contacted at email: tdchuyen@uneti.edu.vn.